Majorana Quasiparticles Protected by $\mathbb{Z}_2$ Angular Momentum Conservation

F. Iemini,[1] L. Mazza,[2] L. Fallani,[3,4] P. Zoller,[5,6] R. Fazio,[1,7] and M. Dalmonte[1]
[1]Abdus Salam International Center for Theoretical Physics, Strada Costiera 11, I-34151 Trieste, Italy
[2]Departement de Physique, Ecole Normale Superieure/PSL Research University, CNRS, 24 rue Lhomond, F-75005 Paris, France
[3]Department of Physics and Astronomy, University of Florence, I-50019 Sesto Fiorentino, Italy
[4]LENS European Laboratory for Nonlinear Spectroscopy, I-50019 Sesto Fiorentino, Italy
[5]Institute for Theoretical Physics, University of Innsbruck, A-6020 Innsbruck, Austria
[6]Institute for Quantum Optics and Quantum Information of the Austrian Academy of Sciences, A-6020 Innsbruck, Austria
[7]NEST, Scuola Normale Superiore and Istituto Nanoscienze-CNR, I-56126 Pisa, Italy
(Received 16 February 2017; published 19 May 2017)

We show how angular momentum conservation can stabilize a symmetry-protected quasitopological phase of matter supporting Majorana quasiparticles as edge modes in one-dimensional cold atom gases. We investigate a number-conserving four-species Hubbard model in the presence of spin-orbit coupling. The latter reduces the global spin symmetry to an angular momentum parity symmetry, which provides an extremely robust protection mechanism that does not rely on any coupling to additional reservoirs. The emergence of Majorana edge modes is elucidated using field theory techniques, and corroborated by density-matrix-renormalization-group simulations. Our results pave the way toward the observation of Majorana edge modes with alkaline-earth-like fermions in optical lattices, where all basic ingredients for our recipe—spin-orbit coupling and strong interorbital interactions—have been experimentally realized over the last two years.

DOI: 10.1103/PhysRevLett.118.200404

Introduction.—The past two decades have witnessed an impressive progress in understanding how to harness quantum systems supporting topological order, one of the ultimate goals being the observation of quasiparticles with non-Abelian statistics—non-Abelian anyons [1–5]. A pivotal role in this search has been the formulation of a model for one-dimensional (1D) p-wave superconductors [6] that supports a symmetry-protected topological phase with Majorana quasiparticles (MQPs) as edge modes. The key element for the stability of such edge modes is the presence of a $\mathbb{Z}_2$ parity symmetry. At the mean-field level, this can be realized via proximity-induced superconductivity in solid-state settings [7–12], or via coupling to molecular Bose-Einsten condensates in cold atoms [13]. Remarkably, it is possible to stabilize MQPs even taking fully into account quantum fluctuations by considering canonical settings [14–18], where the parity symmetry emerges via, e.g., engineered pair tunneling between pairs of wires [19–21]. However, it is an open challenge to understand whether, in these number-conserving setups, there exist *fundamental* microscopic symmetries that can serve as a pristine mechanism for the realization of MQPs, which is genuinely distinct from reservoir-induced superconductivity.

Here, we show how angular momentum conservation enables the realization of a symmetry-protected quasitopological phase supporting MQPs in one-dimensional number-conserving systems [22]. In particular, we show how a combination of spin-exchange interactions and *crossed* spin-orbit couplings in orbital Hubbard models [see Figs. 1(a), 1(b)] naturally gives rise to a $\mathbb{Z}_2$ spin symmetry. This symmetry serves as the enabling tool to realize MQPs, and, as we discuss below, its robustness is guaranteed by the fact that all terms breaking it are not present in the microscopic dynamics, as they would violate angular momentum conservation. Remarkably, these models find direct and natural realization using alkaline-earth-like atoms (AEAs)

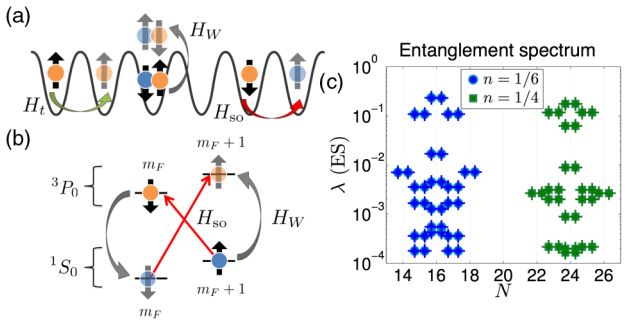

FIG. 1. Schematics of the orbital Hubbard model in the presence of spin-orbit coupling as realized with alkaline-earth-like atoms. (a)–(b) The model we consider in Eq. (1) describes tunneling (H_t), spin-orbit-coupling (H_{so}), and spin-exchange processes (H_W). In cold atom settings, the spin degree of freedom is represented by different Zeeman states with nuclear spin m_F, m_F+1, while the orbital degree of freedom is encoded in different electronic states, $^1S_0$ and $^3P_0$. In these systems, H_W and H_{so} are described by the gray and red arrows, respectively. (c) In the quasitopological phase of the model, the entanglement spectrum displays a characteristic twofold degeneracy: eigenvalues of the reduced density matrix with the same number of particles come in pairs with opposite parities (see text).

in optical lattices [24–32]: in these settings, both spin-exchange interactions [33,34] and spin-orbit couplings [35–37] have already been demonstrated, providing an ideal setting to realize MQPs using state-of-the-art experimental platforms within the paradigm described in the present work.

Model Hamiltonian.—Our starting point is a one-dimensional Hubbard model describing four fermionic species, with annihilation operators $c_{j,\alpha,p}$, with $j \in [1, L]$ a site index, L the length of the system, $\alpha \in [\uparrow, \downarrow]$ describing a pseudospin encoded in a pair of Zeeman states $m_F, m_F + 1$ [depicted in Figs. 1(a), 1(b) as arrows], and $p \in [-1, 1]$ describing orbital degrees of freedom, encoded in the electronic state ground ($^1S_0$, blue) and metastable ($^3P_0$, orange) states. The system Hamiltonian reads

$$H = \sum_j (H_{t,j} + H_{U,j} + H_{W,j} + H_{\mathrm{so},j}); \tag{1}$$

(in the following we also use the notation $H_x = \sum_j H_{x,j}$). The first two terms represent tunneling along the wire, $H_{t,j} = -\sum_{\alpha,p} t(c^\dagger_{j,\alpha,p} c_{j+1,\alpha,p} + \mathrm{H.c.})$, and diagonal interactions, $H_{U,j} = \sum_p U_p n_{j,\uparrow,p} n_{j,\downarrow,p} + U \sum_{\alpha,\beta} n_{j,\alpha,-1} n_{j,\beta,1}$. The third term, visualized by gray arrows in Fig. 1, describes spin-exchange interactions [38]:

$$H_{W,j} = W(c^\dagger_{j,\uparrow,-1} c^\dagger_{j,\downarrow,1} c_{j,\downarrow,-1} c_{j,\uparrow,1} + \mathrm{H.c.}). \tag{2}$$

The last term describes a generalized spin-orbit coupling:

$$H_{\mathrm{so,j}} = \sum_p \{(\alpha_R + b) c^\dagger_{j,\uparrow,p} c_{j+1,\downarrow,-p} + (b - \alpha_R) c^\dagger_{j+1,\uparrow,p} c_{j,\downarrow,-p} + \mathrm{H.c.}\}, \tag{3}$$

where α_R denotes the Rashba velocity, and the b term may be seen as a momentum-dependent Zeeman field [39–41].

In microscopic implementations, the last two terms in H are embodied by strong interorbital spin-exchange interactions (gray arrows) [33,34], and by the possibility of engineering *crossed* spin-orbit couplings (red arrows) via clock lasers [35–37]. The combination of these two ingredients breaks explicitly the global spin-symmetry from $SU(2) \times SU(2)$ down to $\mathbb{Z}_2$—namely, the number of states in each pair of states coupled by spin-orbit coupling is conserved *modulo* 2, due to the presence of the spin-exchange interactions. Indeed, while for $\alpha_R = b = 0$ the Hamiltonian has a $SU(2) \times SU(2)$ spin symmetry [24,25], for generic values of α_R, $b \neq 0$, the spin symmetry is reduced to $\mathbb{Z}_2$, whose correspondent conserved charge is the mutual parity between the two subsets $[(\uparrow, 1), (\downarrow, -1)]$ and $[(\uparrow, -1), (\downarrow, 1)]$ connected by the spin exchange interaction H_W, i.e., $P_m = \mathrm{mod}_2\{[\sum_j (n_{j,\uparrow,1} + n_{j,\downarrow,-1}) - (n_{j,\uparrow,-1} + n_{j,\downarrow,1})]/2\}$. The robustness of this emergent parity symmetry stems from angular momentum conservation: this symmetry may only be broken in the presence of terms such as, e.g., $c^\dagger_{j\uparrow,-1} c_{j,\uparrow,1}$, which generate a quantum of electronic angular momentum while preserving nuclear spin. The mechanism of establishing a $\mathbb{Z}_2$ symmetry is reminiscent of pair hopping of coupled wires [21], although here it emerges naturally, and thus it is experimentally accessible in a physical setting.

This symmetry is the building tool for the realization of a symmetry-protected quasitopological phase whose spin sector has the same universal properties of Kitaev's model—in particular, it hosts MQPs as edge modes. In the following, we discuss the emergence of such a phase using a combination of analytical methods and density-matrix-renormalization-group [42,43] (DMRG) simulations [see Fig. 1(c) for typical entanglement spectrum results, as in the Kitaev model]. We further elucidate the anyon nature of the edge modes by showing how, upon addition of additional four-body interactions, Eq. (1) can be adiabatically connected to a model with exactly soluble ground state properties [19,20], where braiding statistics was recently proved [20].

Low-energy field theory.—In order to underpin the existence of a quasitopological phase supporting MQPs as edge modes, we rely on a field theory based on bosonization [44,45]. Within this framework, the essential point is to identify a sector in the low-energy field theory that displays the same physics of Kitaev's chain. Here, we outline the main steps of our treatment (see Ref. [46] for a detailed treatment). Following conventional bosonization [44,45], we start by replacing each fermionic mode with a pair of right and left movers, $c_{j,\alpha,p} = \psi_{\alpha,p;R}(ja) + \psi_{\alpha,p;L}(ja)$, which are given by

$$\psi_{\alpha,p;r}(x) = \frac{\eta_{\alpha,p;r}}{\sqrt{2\pi a}} e^{i\vartheta_{\alpha,p}} \sum_q e^{irqk_{F,\alpha,p}x} e^{-iqr\varphi_{\alpha,p}} \tag{4}$$

with $r = (-1, 1)$ for L/R, and $\varphi_{\alpha,p}$ and $\vartheta_{\alpha,p}$ being conjugated bosonic operators describing density and phase fluctuations, respectively (a is the lattice spacing). $\eta_{\alpha,p;r}$ are Klein factors, ensuring fermionic commutation relations.

The low-energy Hamiltonian can then be recast into four (three spin, one charge) sectors. The dynamics in these sectors can be understood after applying two canonical transformations: the first one introduces the bosonic fields $\varphi_{f,S/A} = (\varphi_{\uparrow,f} \pm \varphi_{\downarrow,f})/\sqrt{2}$ (and similarly for $\vartheta_{f,S/A}$), with $f = \pm 1$. These bosonic fields describe the behavior of each pair of states coupled by H_{so}: in particular, $\vartheta_{1,S/A}$ and $\vartheta_{-1,S/A}$ describe the $\{c_{\uparrow,1}, c_{\downarrow,-1}\}$ and $\{c_{\uparrow,-1}, c_{\downarrow,1}\}$ pair, respectively. The second transformation considers combinations of these fields in the form

$$\varphi_{f,I} = \frac{\kappa\varphi_{f,S} + \vartheta_{f,A}}{\sqrt{2\kappa}}, \qquad \varphi_{f,II} = \frac{\kappa\varphi_{f,S} - \vartheta_{f,A}}{\sqrt{2}\kappa}, \tag{5}$$

where κ denotes the first harmonic commensurate with the spin-orbit term, and is a function of k_F. After this mapping,

one is left with a gapless charge sector, described by the fields $\vartheta_\rho = \vartheta_{1,II} + \vartheta_{-1,II}/\sqrt{2}$, two gapped spin sectors which play no major role in the dynamics, and a third spin sector, described by the field $\vartheta_\sigma = \vartheta_{1,II} - \vartheta_{-1,II}/\sqrt{2}$, and a Hamiltonian,

$$H_\sigma = \frac{v_\sigma}{2}\int dx\left(\frac{(\partial_x\varphi_\sigma)^2}{K_\sigma} + K_\sigma(\partial_x\vartheta_\sigma)^2\right) + \mathcal{W}\int dx\cos[\sqrt{8\pi}\vartheta_\sigma], \tag{6}$$

with $\mathcal{W} \propto W$, and v_σ, K_σ the sound velocity and Luttinger parameter, respectively. This Hamiltonian describes the low-energy physics of the Kitaev model, to which it can be mapped exactly at the Luther-Emery point $K_\sigma = 2$ [16,21]. It supports a gapless phase for $K_\sigma \leq 1$, and a gapped, topological phase for $K_\sigma > 1$. In the latter, there are two degenerate ground states under open boundary conditions, labeled by different mutual parities $P = \pm 1$: this is possible since the model exhibits a $\mathbb{Z}_2$ symmetry, which serves as a symmetry protection mechanism for the quasitopological phase [46].

In summary, for sufficiently large W/t, the model in Eq. (1) supports a quasitopological phase, with gapless charge excitations, and decoupled gapped spin excitations describing a ground state of a Kitaev model, thus supporting MQPs. The role of additional, diagonal interactions can affect the spin sector [46]: since $K_\sigma - 1 \simeq -(W+U)$, attractive interactions further stabilize the quasitopological phase, while repulsive interactions require larger values of W to open a gap in the spin sector. Equipped with the guideline provided by the low-energy field theory, we present in the following a nonperturbative analysis of the model based on numerical simulations.

DMRG results.—In order to demonstrate the existence of a symmetry-protected quasitopological phase supporting MQPs as edge modes, we employ DMRG simulations based on a rather general decimation prescription for an efficient truncation of the Hilbert space. Typically, we use up to $m = 140$ states, which ensure converge on all observables of interest over all parameter regimes [46]. Following the theoretical discussion above, our analysis is based on four observables: (i) degeneracies in the entanglement spectrum; (ii) finite-size scaling of energy gaps; (iii) bulk decay of correlation functions; and (iv) edge-to-edge correlations. For convenience, we set $t = 1$ as the energy unit.

Given the reduced density matrix ρ_ℓ with respect to a bipartition of the system cutting the ℓth link of the lattice, the entanglement spectrum is the collection of its eigenvalues $\{\lambda_\alpha\}$, and is known to provide striking signatures of topological order via degeneracies [47,48]. In Fig. 1(c), we show typical results for the entanglement spectrum in the quasitopological phase at the representative point $W = -8$, $\alpha_R = b = 4$, $U = 0$ (these features are stable in a broad parameter range [49]). Indeed, the low-lying spectrum displays robust degeneracies for both $n = N/4L = 1/4$ and $n = 1/6$ (with N and L the total numbers of particles and sites, respectively), as expected for a topological phase supporting MQPs edge modes.

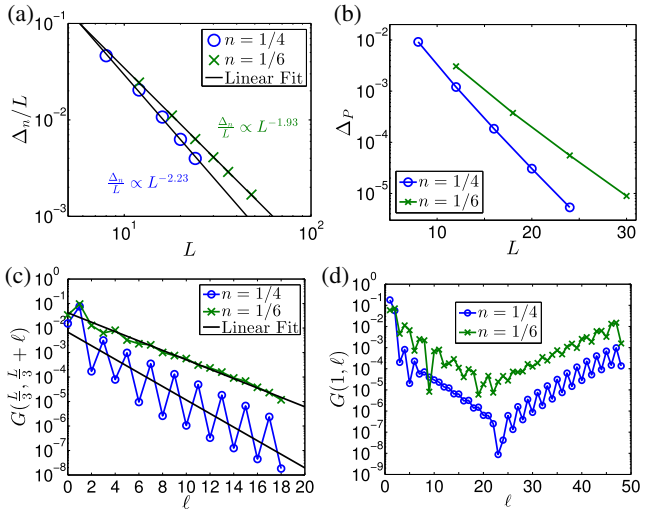

FIG. 2. DMRG analysis of the topological properties of the ground state for model H, at fixed parity, with parameters $W = -8$, $\alpha_R = b = 4$, $U = 0$, at distinct fillings $n = 1/4$ and $n = 1/6$. (a) Algebraic scaling of the gap computed at fixed parity, compatible with $\sim L^{-1}$. (b) Exponential scaling of the gap between the distinct parity sectors. (c)–(d) Single particle correlations $G(j,\ell) = \langle c^\dagger_{j,\uparrow,1} c_{\ell,\uparrow,1}\rangle$ at the bulk (c) and at the edges (d), for a system with $L = 48$ sites.

In Fig. 2(a), we show the decay of the fixed parity gap with open boundary conditions (OBCs), defined as

$$\Delta_n = E^1_L[N,P] - E^0_L[N,P], \tag{7}$$

where $E^n_L[N,P]$ denotes the n-lowest-energy state at size L with number of particles N and mutual parity P. The ground state, with energy $E^0_L[N,P]$, is always in the $P = 1$ sector. In the quasitopological phase, this gap should decay algebraically due to the presence of a gapless charge excitation. This is confirmed by the DMRG results, as shown in Fig. 2(a). Instead, the parity gap

$$\Delta_P = E^0_L[N,-1] - E^0_L[N,1] \tag{8}$$

is sensitive exclusively to spin excitations. As such, it closes exponentially with the system size L, exactly as in the Kitaev chain, as shown in Fig. 2(b).

The presence of a finite bulk gap in the spin sector is signaled by an exponential decay of the Green functions, e.g., $G(j,\ell) = \langle c^\dagger_{j,\uparrow,1} c_{\ell,\uparrow,1}\rangle$, in the bulk [45]. This is portrayed in Fig. 2(c), which shows that coherence is rapidly lost as a function of distance in the bulk.

Crucially, the Green functions are also sensitive to the presence of MQPs edge modes, as these operators locally

switch parity. In Fig. 2(d), we show the correlation of one boundary site with the rest of the chain, $G(1,\ell)$. While the correlation rapidly decays in the bulk due to the presence of a spin gap, there is a strong revival close to the edge of the system, signaling the presence of MQP edge modes. We note that the edge-edge correlation is considerably stronger for filling fractions away from commensurate densities, where the presence of additional (albeit irrelevant) operators is expected to slightly degrade the edge modes, as observed in the Kitaev wire in the presence of repulsive interactions [50,51].

Adiabatic continuity of the ground state to an exactly solvable point.—Remarkably, it is possible to provide direct evidence for the MQP nature of the edge states by showing how the quasitopological phase discussed above is adiabatically connected to the toy model of spinless fermions with exactly solvable ground state properties [19,20], where Ising anyon braiding was recently demonstrated [20].

The strategy to show adiabatic continuity, discussed in detail in Ref. [46], consists of three steps. First, for each pair of states coupled by spin-orbit coupling, we restrict the dynamics to the lower band, following a procedure introduced in Ref. [39,52]. Then, coupling between the lowest bands is introduced via the spin-exchange interaction, and additional four-Fermi couplings. This enlarged Hamiltonian is characterized by two parameters (β,λ): the point (0, 0.9) represents the model studied in the previous section, while the points (1,0.9) and (1,1) represents two points in the phase diagram of the exactly solvable model [19]. We note that all symmetries of the problem are kept for arbitrary (β,λ).

Within this enlarged parameter space, we have carried out DMRG simulations to show that the gap in the spin sector does not close. The latter was extracted from the decay of the Green function in the bulk, $G(j,\ell) \simeq e^{-\alpha_{sp}|j-\ell|}$, and is depicted in Fig. 3(a). Along the full path in parameter space, the gap stays open, implying that our quasitopological state is the same phase as in Ref. [19]. Another striking signature of adiabatic continuity is the fact that all diagnostics applied before signal topological order all along the path. This is illustrated in Fig. 3(b), where we plot the edge-edge Green function at several points along the path itself.

Realization using alkaline-earth-like atoms in optical lattices.—The model discussed above finds a natural implementation using fermionic isotopes of AEA in optical lattices [26], such as ^{171}Yb, ^{173}Yb, and ^{87}Sr. As illustrated in Fig. 1, the orbital degree of freedom is encoded in the electronic state: the $^1S_0$ ground state manifold representing $p=-1$, and the long-lived excited state manifold $^3P_0$ representing $p=1$. The spin degree of freedom is instead encoded in the nuclear spin state, which for AEA is basically decoupled from the electronic degree of freedom for both the ground and low-lying excited states. In ^{171}Yb, the nuclear spin is $I=1/2$, so all degrees of freedom are immediately available as required here. For ^{173}Yb and ^{87}Sr, which do have $I=5/2$ and $9/2$, respectively, unwanted

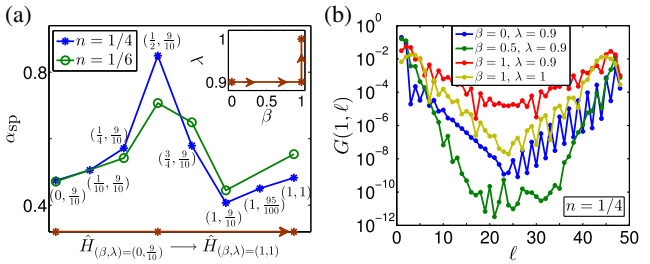

FIG. 3. DMRG analysis for the adiabatic continuity of model H to an exactly solvable model. (a) Parity gap "α_{sp}" along the adiabatic continuity path $(\beta=0,\lambda=9/10)\rightarrow(\beta=1,\lambda=1)$. Inset illustrates the Hamiltonian parameters varied along the path. (b) Single particle edge correlations along the adiabatic path—similar behavior follows for $n=1/6$. In all plots we consider a system with $L=48$ sites and use $m=140$ number of kept states in the DMRG simulations.

Zeeman states can be excluded from the dynamics either employing state-dependent light shifts [31], or by exploiting the fact that the clock frequency is m_F dependent due to different linear Zeeman shifts in the $^1S_0$ and $^3P_0$ manifold.

The two key elements of our proposal, large spin-exchange interactions and spin-orbit couplings on the so-called clock transition, build upon state-of-the-art experimental progresses in AEA physics. As demonstrated in recent experiments with ^{173}Yb [33,34], the spin-exchange interaction in these settings can be extremely large, of the order of $5/10$ kHz in optical lattices, guaranteeing that the driven interaction strength in our system is considerably larger than typical temperatures. Moreover, the ratio W/t can be tuned via modifying either the optical lattice depth or the trapping in the transverse direction. Spin-orbit coupling between ground and excited states has been recently demonstrated both at JILA [37] and at LENS [36] realizing single-particle band structures akin to the one employed here, albeit with slightly different microscopic Hamiltonians (following Ref. [39], the precise form we use here requires a tilting of the lattice or a superlattice structure). In concrete, considering typical tunneling rates of order $t\simeq 100h$ Hz, spin-orbit couplings of order $400h$ Hz and spin-exchange interactions of order $800h$ Hz would give direct access to the quasitopological phase. In these experimental settings, the quasitopological phase can be characterized using both correlation function and spectral properties, as discussed above. The nature of the edge modes can be demonstrated using a variety of techniques [55]. In particular, time-of-flight imaging and edge spectroscopy can be used to demonstrate the existence of zero-energy modes and their inherent correlations. Moreover, the fact that our model is adiabatically connected to an exactly solvable point provides a qualitative guidance on the shape of the MQP wave function—generically hard to analytically access in interacting systems—opening up a concrete perspective to realize braiding operations in such settings.

Conclusions.—We have shown how Majorana quasiparticles can emerge as edge modes of orbital Hubbard models in the presence of spin-orbit interactions. The key element for the realization of the quasitopological phase supporting them is angular momentum conservation, an epitome building block of atomic physics experiments. The stability of the mechanism we propose paves the way toward the investigation of interacting topological states and Majorana edge modes in both atomic clocks and optical lattice experiments, where the main ingredients of our proposal are naturally realized and have been experimentally demonstrated over the last two years.

The numerical part of this work has been performed using the DMRG code released within the "Powder with Power" project [56].

We acknowledge useful discussions with M. A. Baranov, J. Catani, D. Rossini, and C. Sias. This work is partly supported by EU-IP-QUIC (R. F.), the ERC Synergy grant UQUAM (P. Z.), and the ERC Consolidator grant TOPSIM (L. F.). L. M. was supported by LabEX ENS-ICFP: ANR-10- LABX-0010/ANR-10-IDEX-0001-02 PSL*. This work was granted access to the HPC resources of MesoPSL financed by the Region Ile de France and the project Equip@Meso (reference ANR-10-EQPX-29-01).

Note added.—While completing this work, a Ref. [57] appeared, where the commensurate regime of a model combining spin-exchange interactions with a different type of spin-orbit coupling was investigated.

[1] C. Nayak, S. H. Simon, A. Stern, M. Freedman, and S. Das Sarma, Rev. Mod. Phys. **80**, 1083 (2008).
[2] F. Wilczek, Nat. Phys. **5**, 614 (2009).
[3] J. Alicea, Rep. Prog. Phys. **75**, 076501 (2012).
[4] C. W. J. Beenakker, Annu. Rev. Condens. Matter Phys. **4**, 113 (2013).
[5] N. Goldman, J. C. Budich, and P. Zoller, Nat. Phys. **12**, 639 (2016).
[6] A. Kitaev, Phys. Usp. **44**, 131 (2001).
[7] V. Mourik, K. Zou, S. M. Frolov, S. R. Plissard, E. P. A. M. Bakkers, and L. P. Kouwenhoven, Science **336**, 1003 (2012).
[8] M. T. Deng, C. L. Yu, G. Y. Huang, M. Larsson, P. Caroff, and H. Q. Xu, Nano Lett. **12**, 6414 (2012).
[9] A. Das, Y. Ronen, Y. Most, Y. Oreg, M. Heiblum, and H. Shtrikman, Nat. Phys. **8**, 887 (2012).
[10] L. P. Rokhinson, X. Liu, and J. K. Furdyna, Nat. Phys. **8**, 795 (2012).
[11] S. Nadj-Perge, I. K. Drozdov, J. Li, H. Chen, S. Jeon, J. Seo, A. H. MacDonald, B. A. Bernevig, and A. Yazdani, Science **346**, 602 (2014).
[12] S. M. Albrecht, A. P. Higginbotham, M. Madsen, F. Kuemmeth, T. S. Jespersen, J. Nygård, P. Krogstrup, and C. M. Marcus, Nature (London) **531**, 206 (2016).
[13] L. Jiang, T. Kitagawa, J. Alicea, A. R. Akhmerov, D. Pekker, G. Refael, J. I. Cirac, E. Demler, M. D. Lukin, and P. Zoller, Phys. Rev. Lett. **106**, 220402 (2011).
[14] G. Ortiz, J. Dukelsky, E. Cobanera, C. Esebbag, and C. Beenakker, Phys. Rev. Lett. **113**, 267002 (2014).
[15] C. Chen, W. Yan, C. S. Ting, Y. Chen, and F. J. Burnell, arXiv:1701.01794.
[16] M. Cheng and H.-H. Tu, Phys. Rev. B **84**, 094503 (2011).
[17] L. Fidkowski, R. M. Lutchyn, C. Nayak, and M. P. A. Fisher, Phys. Rev. B **84**, 195436 (2011).
[18] J. D. Sau, B. I. Halperin, K. Flensberg, and S. Das Sarma, Phys. Rev. B **84**, 144509 (2011).
[19] F. Iemini, L. Mazza, D. Rossini, R. Fazio, and S. Diehl, Phys. Rev. Lett. **115**, 156402 (2015).
[20] N. Lang and H. P. Büchler, Phys. Rev. B **92**, 041118 (2015).
[21] C. V. Kraus, M. Dalmonte, M. A. Baranov, A. M. Läuchli, and P. Zoller, Phys. Rev. Lett. **111**, 173004 (2013).
[22] Quasitopological phases include a topological, gapped sector, in addition to decoupled gapless modes; see Refs. [21,23].
[23] P. Bonderson and C. Nayak, Phys. Rev. B **87**, 195451 (2013).
[24] M. A. Cazalilla, A. F. Ho, and M. Ueda, New J. Phys. **11**, 103033 (2009).
[25] A. V. Gorshkov, M. Hermele, V. Gurarie, C. Xu, P. S. Julienne, J. Ye, P. Zoller, E. Demler, M. D. Lukin, and A. M. Rey, Nat. Phys. **6**, 289 (2010).
[26] M. A. Cazalilla and A. M. Rey, Rep. Prog. Phys. **77**, 124401 (2014).
[27] S. Stellmer, M. K. Tey, B. Huang, R. Grimm, and F. Schreck, Phys. Rev. Lett. **103**, 200401 (2009).
[28] B. J. DeSalvo, M. Yan, P. G. Mickelson, Y. N. Martinez de Escobar, and T. C. Killian, Phys. Rev. Lett. **105**, 030402 (2010).
[29] S. Sugawa, K. Inaba, S. Taie, R. Yamazaki, M. Yamashita, and Y. Takahashi, Nat. Phys. **7**, 642 (2011).
[30] M. D. Swallows, M. Bishof, Y. Lin, S. Blatt, M. J. Martin, A. M. Rey, and J. Ye, Science **331**, 1043 (2011).
[31] M. Mancini, G. Pagano, G. Cappellini, L. Livi, M. Rider, J. Catani, C. Sias, P. Zoller, M. Inguscio, M. Dalmonte, and L. Fallani, Science **349**, 1510 (2015).
[32] C. Hofrichter, L. Riegger, F. Scazza, M. Höfer, D. R. Fernandes, I. Bloch, and S. Folling, Phys. Rev. X **6**, 021030 (2016).
[33] G. Cappellini *et al.*, Phys. Rev. Lett. **113**, 120402 (2014).
[34] F. Scazza, C. Hofrichter, M. Höfer, P. C. De Groot, I. Bloch, and S. Fölling, Nat. Phys. **10**, 779 (2014).
[35] M. L. Wall, A. P. Koller, S. Li, X. Zhang, N. R. Cooper, J. Ye, and A. M. Rey, Phys. Rev. Lett. **116**, 035301 (2016).
[36] L. F. Livi *et al.*, Phys. Rev. Lett. **117**, 220401 (2016).
[37] S. Kolkowitz, S. L. Bromley, T. Bothwell, M. L. Wall, G. E. Marti, A. P. Koller, X. Zhang, A. M. Rey, and J. Ye, Nature (London) **542**, 66 (2017).
[38] These interactions are quasiresonant up to intermediate values of the external magnetic field.
[39] J. C. Budich, C. Laflamme, F. Tschirsich, S. Montangero, and P. Zoller, Phys. Rev. B **92**, 245121 (2015).
[40] The b term is not fundamental to stabilize MQPs, but considerably simplifies a part of the theoretical analysis below.
[41] J. C. Budich and E. Ardonne, Phys. Rev. B **88**, 035139 (2013).
[42] S. R. White, Phys. Rev. Lett. **69**, 2863 (1992).

[43] U. Schollwöck, Rev. Mod. Phys. **77**, 259 (2005).
[44] A. O. Gogolin, A. A. Nersesyan, and A. M. Tsvelik, *Bosonization and Strongly Correlated Systems* (Cambridge University Press, Cambridge, England, 1998).
[45] T. Giamarchi, *Quantum Physics in One Dimension* (Oxford University Press, Oxford, 2003).
[46] See supplemental material at http://link.aps.org/supplemental/10.1103/PhysRevLett.118.200404, including details on the low-energy field theory.
[47] F. Pollmann, A. M. Turner, E. Berg, and M. Oshikawa, Phys. Rev. B **81**, 064439 (2010).
[48] A. M. Turner, F. Pollmann, and E. Berg, Phys. Rev. B **83**, 075102 (2011).
[49] M. Dalmonte *et al.* (to be published).
[50] E. M. Stoudenmire, J. Alicea, O. A. Starykh, and M. P. A. Fisher, Phys. Rev. B **84**, 014503 (2011).
[51] M. Tezuka and N. Kawakami, Phys. Rev. B **85**, 140508(R) (2012).
[52] This passage is reminiscent of treating the orbital degrees of freedom as a synthetic dimension [31,53,54].
[53] A. Celi, P. Massignan, J. Ruseckas, N. Goldman, I. B. Spielman, G. Juzeliunas, and M. Lewenstein, Phys. Rev. Lett. **112**, 043001 (2014).
[54] B. K. Stuhl, H.-I. Lu, L. M. Aycock, D. Genkina, and I. B. Spielman, Science **349**, 1514 (2015).
[55] C. V. Kraus, S. Diehl, P. Zoller, and M. A. Baranov, New J. Phys. **14**, 113036 (2012).
[56] See http://qti.sns.it/dmrg/home.html.
[57] X. Zhou *et al.*, arXiv:1612.08880.